Chemistry & Biology
Article

Characterization of a Proteolytically Stable Multifunctional Host Defense Peptidomimetic

Rasmus D. Jahnsen,[1,2] Evan F. Haney,[2] Henrik Franzyk,[1,*] and Robert E.W. Hancock[2,*]
[1]Department of Drug Design and Pharmacology, Faculty of Health and Medical Sciences, University of Copenhagen, Universitetsparken 2, Copenhagen DK-2100, Denmark
[2]Centre for Microbial Diseases and Immunity Research, University of British Columbia, 2259 Lower Mall Research Station, Vancouver, BC V6T 1Z4, Canada
*Correspondence: henrik.franzyk@sund.ku.dk (H.F.), bob@hancocklab.com (R.E.W.H.)
http://dx.doi.org/10.1016/j.chembiol.2013.09.007

SUMMARY

The in vitro activity of a host defense peptidomimetic (HDM-4) was investigated. The compound exhibited an antimicrobial activity profile against a range of Gram-negative bacteria. HDM-4 permeabilized the outer membrane and partly depolarized the inner membrane at its minimal inhibitory concentration (MIC). Moreover, it was demonstrated that HDM-4 was distributed widely in the bacterial cell at lethal concentrations, and that it could bind to DNA. It was confirmed that the multimodal action of HDM-4 resulted in it being less likely to lead to resistance development as compared to single-target antibiotics. HDM-4 exhibited multispecies anti-biofilm activity at sub-MIC levels. Furthermore, HDM-4 modulated the immune response by inducing the release of the chemoattractants interleukin-8 (IL-8), monocyte chemotactic protein-1 (MCP-1), and MCP-3 from human peripheral blood mononuclear cells. In addition, the compound suppressed lipopolysaccharide-mediated inflammation by reducing the release of the pro-inflammatory cytokines IL-6 and tumor necrosis factor-α.

INTRODUCTION

Reports of the emergence of resistance development among pathogenic bacterial strains continue to increase. Infectious diseases will become increasingly less treatable with conventional antibiotics and thus new clinical strategies are urgently needed (Theuretzbacher, 2013). At the same time, there is a declining effort from pharmaceutical companies in pursuing the development of new classes of anti-infective agents, and few new antibacterial agents are being approved in the United States (Boucher et al., 2009; Jabes, 2011). Thus, to solve this persistent health problem, the research and development of new anti-infective agents constitutes an important task for academic institutions. Antimicrobial host defense peptides (HDPs) have for many years been considered lead compounds for novel antibiotics (Brogden, 2005; Hancock and Sahl, 2006; Mookherjee and Hancock, 2007). However, after 30 years of efforts, synthetic antimicrobial peptides have had very limited success. General problems encountered are typically toxicity, cost of raw materials, and susceptibility toward enzymatic degradation (Fjell et al., 2012; Hancock and Sahl, 2006).

In this study, we characterized the in vitro activity of a proteolytically stable simple host defense peptidomimetic (HDM-4) with low toxicity toward mammalian cells. We showed that HDM-4 counteracted Gram-negative pathogens in a multifunctional manner through membrane disruption and DNA binding. Additionally, HDM-4 promoted immunomodulatory anti-infective functions by inducing chemokines in immune cells and inhibiting lipopolysaccharide (LPS)-induced pro-inflammatory responses.

RESULTS

Spectrum of Activity and Killing Kinetics

We previously reported that HDM-4 exhibits low toxicity against red blood cells and HeLa cells as well as high antibacterial activity against *E. coli* multidrug-resistant strains including ESBL and NDM-1 producers (Jahnsen et al., 2012). The activity against additional Gram-negative bacteria was investigated (Table 1). Several HDPs reported in the literature were included in the screen: polymyxin B (Storm et al., 1977), a polypeptide isolated from *Bacillus polymyxus*; IDR-1018 (Wieczorek et al., 2010), a synthetic short cationic immunomodulating peptide with weak direct antibacterial activity; CRAMP (Gallo et al., 1997), a natural cathelin-related murine antimicrobial peptide; and bovine bactenecin derivatives Bac2A and W3 (Hilpert et al., 2005; Wieczorek et al., 2010).

HDM-4 exhibited broad-spectrum activity at levels (minimum inhibitory concentration [MIC] $\leq$ 10 μM) comparable to many of the known HDPs (Table 1). In particular, the growth of *E. coli* and *K. pneumoniae* was inhibited at low concentrations. The killing kinetics of *E. coli* exposed to HDM-4 were compared to those observed for several clinically applied antibiotics, and HDM-4 was investigated at various concentrations (Figure 1).

At 4-fold the MIC, HDM-4 killed *E. coli* more rapidly than other antibiotics commonly used in the clinic (Figure 1). Antimicrobial HDPs are proposed to exert their direct bacterial killing by a multimodal mechanism of action involving combinations of disruption of membrane barrier function, antagonism of biosynthetic processes that involve cytoplasmic membrane-associated enzymes, internalization, and action on cytosolic targets (Fjell et al., 2012; Hale and Hancock, 2007). Thus, upon reaching a threshold concentration, peptides accumulated at the lipid bilayer can rapidly cause cell death as previously shown for polymyxin B (HsuChen and Feingold, 1973). Notably, HDM-4 acted

Table 1. Antibacterial Activity of HDM-4

Compound/Strain	MIC [μg/ml] (μM)				
	E. coli	*P. aeruginosa*	*S. enterica* Typhimurium	*A. baumannii*	*K. pneumoniae*
HDM-4	4 (1.3)	32 (10)	32 (10)	32 (10)	0.5 (0.2)
Polymyxin B	2 (1.4)	1 (0.7)	0.5 (0.4)	16 (11)	2 (1.4)
IDR-1018	32 (15)	>64 (>30)	16 (7.6)	16 (7.6)	2 (0.9)
CRAMP	32 (8.4)	>64 (>17)	>64 (>17)	>64 (>17)	32 (8.4)
Bac2A	32 (23)	>64 (>45)	>64 (>45)	>64 (>45)	4 (2.8)
W3	16 (10)	>64 (>41)	32 (>21)	16 (10)	2 (1.3)

The MIC of HDM-4 against several clinically important Gram-negative pathogens.

more slowly than polymyxin B (Figure 1), and at low concentrations, the killing took place within hours after an initial lag phase. These observations suggest that alternative more "slow-acting" mechanisms other than membrane disruption are involved for HDM-4, most likely implicating inhibition of essential metabolic functions including DNA, RNA, or protein synthesis (Hale and Hancock, 2007).

Mode of Action

To further elucidate the antibacterial mode of action, the effects of HDM-4 on *E. coli* were investigated using a range of microscopic and spectroscopic methods as well as functional assays (Figure 2).

Effects on the outer membrane of *E. coli* were demonstrated with field emission scanning-electron microscopy (Figure 2B). At the MIC, the micrographs clearly showed membrane damage including blebs, especially localized at the end of the bacterial rod. The disruptive effects were more pronounced with increased concentration, which corresponded well to the concentration-dependent killing rate observed in Figure 1B. General morphologic changes were observed at all concentrations, but extensive leakage of intracellular material was only detected at higher concentrations (32 μg/ml; 8× MIC), and even at this concentration cells generally maintained their shapes, indicating a lack of lysis, and thereby corroborating the assumption that intracellular targets may be involved at the MIC. Outer membrane permeabilization of *E. coli* O157:H7 was measured with the 1-N-phenylnapthylamine (NPN) assay (Loh et al., 1984) with polymyxin B as a positive control (Figure 2C). At the MIC (4 μg/ml), HDM-4 caused 75% permeabilization relative to excess polymyxin B. Inner membrane depolarization was then measured using the $diSC_3$-5 assay (Wu et al., 1999) with the membrane-active peptide melittin as a positive control (Figure 2D). To eliminate interference from the outer membrane in uptake of $diSC_3$-5, an *E. coli* (DC2) strain with a weakened outer membrane was used in this assay. The MIC toward this strain was 2-fold higher than that against the O157:H7 strain, consistent with the possibility that outer membrane permeabilization in *E. coli* was not rate-limiting for HDM-4 action. A strong concentration-dependent activity was observed, but the effect was most pronounced at sub-MIC levels. Nevertheless, at the MIC (8 μg/ml) only 42% depolarization relative to that of excess melittin was observed. Interestingly, further addition of HDM-4 resulted in a more moderate increase in depolarization, while complete depolarization required 10× MIC (40 μg/ml). These data were thus consistent with the suggestion that mechanisms other than inner membrane disruption were involved in killing at the MIC.

To investigate a putative intracellular mechanism for HDM-4, a TAMRA-labeled derivative (Figure 2A) was synthesized. To examine the potential impact of the altered physicochemical properties of the labeled compound on its activity, the bacterial killing ability of TAMRA-HDM-4 was compared to that of native HDM-4 (Figure 2E). Labeling the compound resulted in a 2-fold increase in MIC as compared to the original compound. An examination of the killing kinetics (adjusted for the difference in MIC) showed comparable time-kill curves during treatment with 8× MIC. The distribution of TAMRA-HDM-4 in bacterial cells after 30 min was depicted with confocal imaging (Figure 2F). At 0.5× MIC (4 μg/ml) TAMRA-HDM-4 localized only in the membrane, and mainly at the ends of the bacterial rods, whereas general distribution into most parts of the cells was observed at the MIC (i.e., 8 μg/ml). At 4× MIC (32 μg/ml), the membranes were extensively perturbed, and TAMRA-HDM-4 was present also in the area surrounding the bacterial cells. To investigate the capability of HDM-4 for binding intracellular components such as DNA, a gel-retardation assay (Haney et al., 2013) was performed (Figure 2G). Inhibition of plasmid migration in the agarose gel was detectable at a HDM-4:plasmid weight ratio of 2:1, with complete inhibition observed at ratios greater than 3:1.

Resistance Development against HDM-4 in *E. coli*

An evaluation of the ability of HDM-4 to induce resistance development in *E. coli* upon long-term exposure was carried out (Figure 3).

Because HDM-4 appeared to act via multiple non-specific targets, it was expected that resistance upon repetitive sub-MIC treatment would be less likely to occur for HDM-4 as compared to conventional antibiotics having a single specific target. The investigation indeed demonstrated that *E. coli*, when exposed to sub-lethal concentrations for 20 cycles, exhibited a higher relative susceptibility to HDM-4 than to representatives of the major antibiotic classes including aminoglycosides (gentamicin), carbapenems (imipenem), cephalosporins (cefotaxime), and fluoroquinolones (ciprofloxacin). Only polymyxin B demonstrated a lower tendency for resistance development because the MIC remained constant after 20 cycles. At least an 8-fold increase in the MIC was obtained for the tested conventional antibiotics, whereas only a 2-fold increase was observed for HDM-4. The resistance properties were not caused by adaptive resistance, as the treated bacteria were grown for additional two cycles

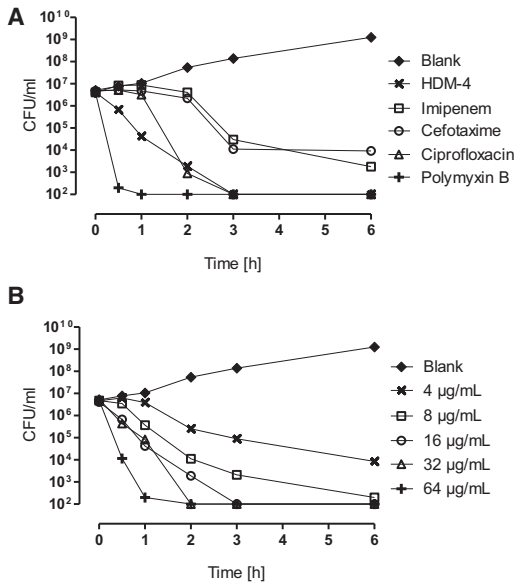

Figure 1. Killing Kinetics

(A) Time-kill study of *E. coli* O157:H7 exposed to various antibacterials. Cultures in log phase at 3.5 × 10^6 to 5.5 × 10^6 CFU/ml were challenged with 4 × MIC; all numbers recorded as 10^2 had ≤100 CFU/ml.

(B) Time-kill study of *E. coli* O157:H7 exposed to HDM-4 at various concentrations relative to the MIC of 4 μg/ml. The experiment was performed three times and one representative curve for each concentration is shown.

without treatment and compared anew; the lower susceptibility of the population was still present.

Broad-Spectrum Antibiofilm Activity

It was recently demonstrated that small synthetic cationic peptides are able to disrupt bacterial biofilm formation (de la Fuente-Núñez et al., 2012). A screening for inhibition of biofilm formation by different Gram-negative bacteria was performed (Figure 4A). The planktonic MICs in biofilm medium were in two cases slightly different as compared to those obtained in the standard MIC assay medium, being 16–64 μg/ml. Interestingly, inhibition of biofilm formation at sub-MIC concentrations was found for all investigated bacteria. In particular, biofilm growth for *P. aeruginosa* and *A. baumannii* was diminished significantly even at a concentration 8-fold lower than the MIC. For all strains, the biomass was reduced by > 90% at 16 μg/ml (i.e., at 0.125–0.5× planktonic cell MIC).

More details about the antibiofilm activity were obtained by subjecting *P. aeruginosa* to flow cell-based biofilm investigations (Figure 4B). Bacteria were allowed to adhere to a glass surface for 2 hr. Subsequently, a continuous flow of medium containing 0.125× MIC of HDM-4 was applied for 6 days. The biofilm was live/dead stained and visualized with confocal microscopy. In the untreated control, a ''lawn-like'' biofilm with well-defined microcolony structures was seen, and electron microscopy imaging showed a smooth biofilm surface comprising many cells with healthy morphology. In contrast, the treated sample exhibited a majority of dead cells as revealed by staining with both the general stain Syto-9 Green and the normally impermeant stain propidium iodide. A ''lawn-like'' biofilm structure was absent, but well-defined microcolonies were readily detected, albeit that the majority of cells were dead, especially at the core of the biofilm colonies. Electron microscopy revealed smooth bacterial cell surfaces and a relatively high abundance of extracellular polymeric matrix.

Immune Response Modulation

There is evidence that certain host defense peptides (e.g., the human cathelicidin LL-37) also participate in the innate immune response to infections by stimulating chemokine release, thereby mobilizing the immune system (Scott et al., 2002). Synthetic peptides have been designed to mimic and accentuate this activity (Scott et al., 2007). Human peripheral blood mononuclear cells (PBMCs) were stimulated with HDM-4 to investigate its ability to induce production of the neutrophil chemokine interleukin 8 (IL-8; CXCL8) as well as the monocyte chemotactic proteins MCP-1 and MCP-3 (also termed CCL2 and CCL7, respectively, because they belong to the subfamily of CC chemokines). The strongly immunomodulatory peptide IDR-1018 (Wieczorek et al., 2010) was included as a positive control. The cytotoxic effects of IDR-1018 and HDM-4 were investigated with the lactate dehydrogenase (LDH) assay (Decker and Lohmann-Matthes, 1988) at relevant concentrations prior to chemokine investigations. At 20 μg/ml, HDM-4 and IDR-1018 demonstrated 7.5 ± 6.7% and 2.2 ± 4.7% LDH release, respectively. At 50 μg/ml, the release was 10.3 ± 7.8% and ~0%, respectively.

As expected, a strong induction of chemokines was observed for IDR-1018 at both concentrations tested (Figure 5A). No significant chemokine induction was detected for HDM-4 at 20 μg/ml, however, when stimulating with 50 μg/ml, significant induction of all chemokines to levels comparable to those seen for low-dose IDR-1018 treatment was observed.

In response to the bacterial outer-membrane component LPS, the monocytes of infected hosts excrete excessive amounts of pro-inflammatory mediators, like the cytokines IL-6 and tumor necrosis factor-α (TNF-α), that can be harmful and lead to a potentially lethal systemic inflammatory response syndrome (Davies and Hagen, 1997). LL-37 and certain synthetic peptides are known to inhibit the LPS-induced release of pro-inflammatory cytokines through a complex mechanism (Mookherjee et al., 2006; Turner-Brannen et al., 2011). In addition, it has been shown that short cationic peptides exert an inhibitory effect on the LPS-induced inflammatory response by blocking the interaction between LPS and LPS-binding protein (Scott et al., 2000). The ability of HDM-4 to inhibit the LPS-mediated pro-inflammatory response was investigated (Figure 5B), and its LPS-binding properties were determined (Figure 5C). Because IDR-1018 has been previously shown to strongly inhibit the pro-inflammatory response (Wieczorek et al., 2010), it was included as a positive control in addition to polymyxin B. Treatment with the compounds alone did not induce significant levels of IL-6 or TNF-α (data not shown). Addition of HDM-4 together with LPS inhibited the release of TNF-α and IL-6 from PBMCs. For TNF-α, both HDM-4 and IDR-1018 completely abolished the cytokine signal, whereas for IL-6, low levels of cytokine could still be detected, with HDM-4 being slightly more efficient than IDR-1018. Both compounds exhibited concentration-dependent fluorophore displacement from LPS, with HDM-4 being slightly more active. Polymyxin B gave rise to a stronger displacement than that seen with both test compounds.

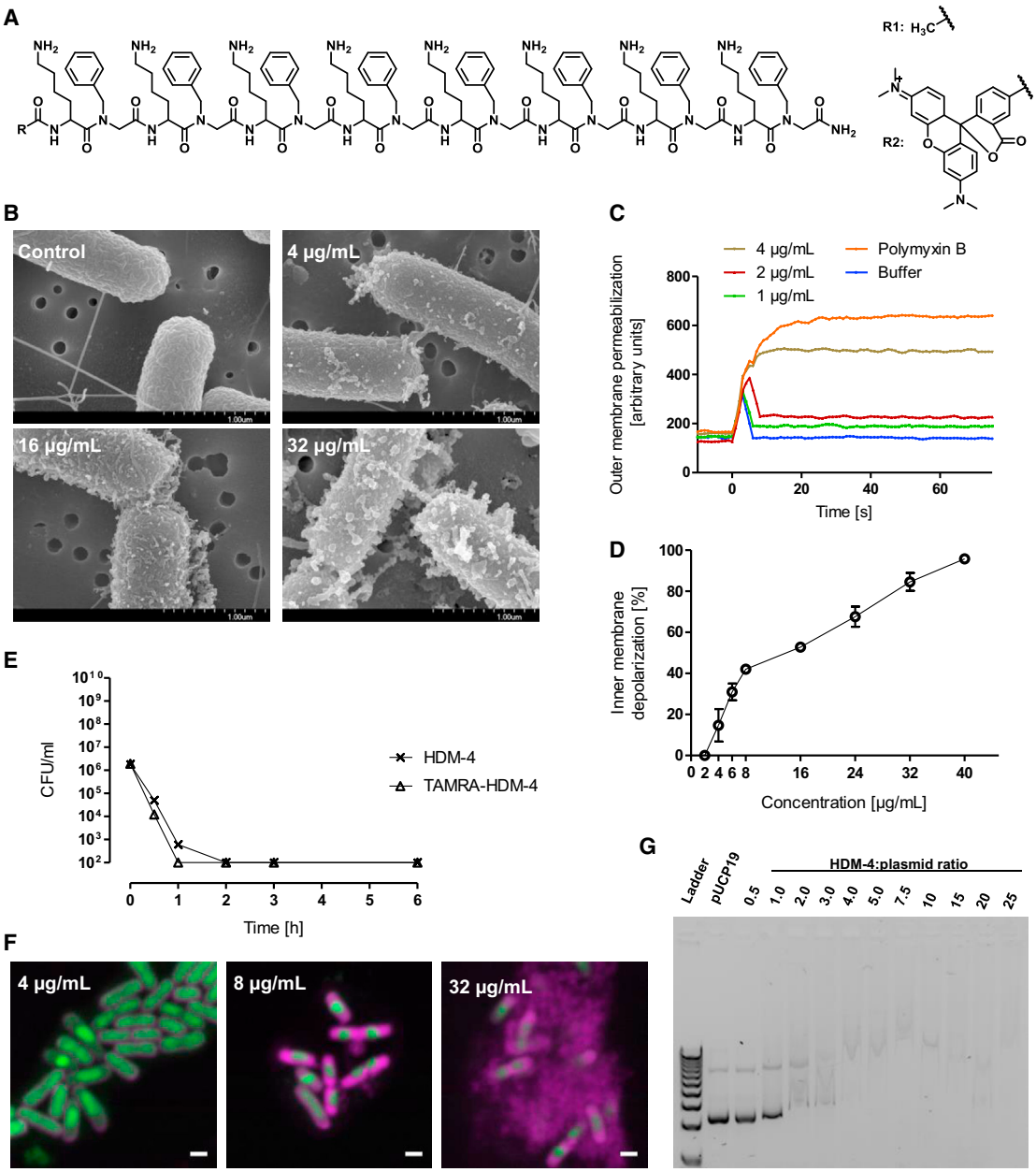

Figure 2. Investigations of the Antibacterial Mode of Action of HDM-4

(A) Structure of native HDM-4 (**R1**) and TAMRA-labeled HDM-4 (**R2**).

(B) Scanning-electron micrographs of *E. coli* O157:H7 exposed to HDM-4 at various concentrations relative to the MIC of 4 µg/ml. Cultures in log phase (3.0–4.0 × 10^7 CFU/ml) were treated for 30 min prior to fixation and sample preparation.

(C) Outer membrane damage of *E. coli* O157:H7 at low HDM-4 concentrations. At time zero, test compounds were added to the sample. Excess polymyxin B (6.4 µg/ml) demonstrated complete permeabilization. At the MIC (4 µg/ml), ~75% permeabilization relative to polymyxin B was observed. The experiment was performed three times and one representative curve for each concentration is shown.

(D) Concentration-dependent cytoplasmic membrane depolarization of *E. coli* (DC2). The results are presented as mean % depolarization ± SD of three independent experiments assessed relative to that of excess melittin (20 µM = 57 µg/ml). The MIC of HDM-4 against *E. coli* (DC2) was 8 µg/ml and led to a 42% depolarization. Data are represented as mean ± SEM.

(E) Time-kill kinetics for *E. coli* (O157:H7) exposed to native HDM-4 and TAMRA-labeled HDM-4 (MIC = 8 µg/ml). Cultures in log phase at 3.5–5.5 × 10^6 CFU/ml were challenged with 4 × MIC; all counts ≤ 100 CFU/ml are depicted as 10^2 CFU/ml. The experiment was performed three times and one representative curve for each concentration is shown.

(F) Confocal micrographs of *E. coli* (O157:H7) after exposure to TAMRA-labeled HDM-4 (false-colored magenta) at various concentrations and counterstaining with the DNA fluorescent stain 4′,6-diamidino-2-phenylindole (DAPI) (false-colored green). Cultures in log phase (3.9 × 10^7 CFU/mL) were treated for 30 min prior to fixation and sample preparation. The scale bars represent 1 µm. An untreated control was examined to confirm that no background fluorescence was present (data not shown).

(G) Inhibition of plasmid pUCP19 DNA migration on a 1% agarose gel at different HDM-4:plasmid weight ratios.

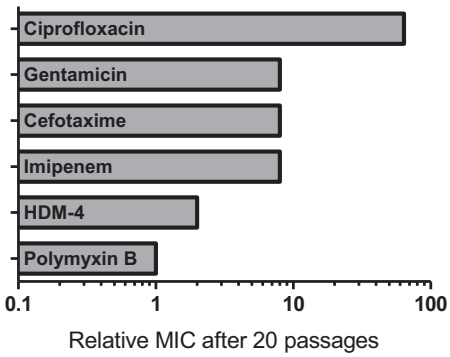

Figure 3. Resistance Development Induced by Antibacterial Agents
Development of resistance in *E. coli* (O157:H7) after 20 consecutive passages continuously treated with antibiotics or HDM-4 at sublethal levels. The relative MIC is the ratio of the MIC obtained for a given subculture exposed for 20 passages relative to that observed during the first passage.

DISCUSSION

Multidrug-resistant bacteria are becoming increasingly prevalent. As recently as a decade ago, most of these organisms posed little health risk, as they could be treated with one or more conventional antibiotics. Today, the situation has changed dramatically, and, in particular, Gram-negative bacteria like *E. coli, Pseudomonas*, *Klebsiella*, and *Acinetobacter* spp. are considered severe threats to public health (Oteo et al., 2010). In the present work, we have extensively characterized the antimicrobial activity and mechanism of action of HDM-4, a nontoxic peptidomimetic with potent broad-spectrum antibacterial activity against a range of Gram-negative species. We propose that HDM-4 may combat bacterial infections in a multifunctional manner and thus, bacterial killing takes place as the result of an overall mode of action involving cell membrane perturbation and binding to intracellular components such as bacterial DNA. In addition, the immunomodulatory properties of HDM-4 could lead to enhanced bacterial clearance by the cells of the host immune system, resulting in a multipronged attack against invading pathogens. HDPs have been called "dirty drugs" because they often interact with several low-affinity targets rather than blocking a single high-affinity target, ultimately limiting co-evolution of HDPs and bacterial resistance (Peschel and Sahl, 2006). This is supported by the present results because assessment of resistance development demonstrated that both polymyxin B and HDM-4 remained highly active against *E. coli* after continuous treatment with subinhibitory concentrations, in contrast to all tested conventional antibiotics. Still, bacterial resistance toward HDPs has been observed previously due to several defense strategies including altered membrane composition, active efflux, and enzymatic degradation. In the latter case, it has been shown that the human cathelicidin LL-37 is inactivated via proteolytic degradation by *S. aureus* (Sieprawska-Lupa et al., 2004). The peptidomimetic structure of HDM-4 is not recognized by proteolytic enzymes providing HDM-4 with an advantage as compared to HDPs composed exclusively of α-amino acids, both with respect to resistance and stability in the face of host proteases that abound during infections.

Importantly, evidence suggests that HDPs generally exert their natural anti-infective functions mainly through immune modulation (Bowdish et al., 2005). Not surprisingly, this is an advantage in the context of resistance development as such an indirect activity relieves selection pressure. It could be argued that a potential anti-infective drug candidate with multiple mechanisms including direct (i.e., bacterial killing) and indirect (i.e., immune modulation) killing has a higher potential for success in the clinic with reduced resistance development when compared to single-mechanism antibiotics. In the present in vitro investigation, it was demonstrated that HDM-4 constitutes one such candidate.

One way for bacteria to adapt to inhospitable environments involves biofilm formation, which is a microbiological process that is associated with ~65% of all human infections and is linked to increased pathogenesis and multidrug resistance (Costerton et al., 1999; Donlan, 2001; Parsek and Singh, 2003). Biofilms are highly abundant in certain infectious diseases, e.g., *P. aeruginosa* biofilms in the lungs of patients with cystic fibrosis (Römling and Balsalobre, 2012; Singh et al., 2000). As previously described, peptoids and peptide-peptoid hybrids may be efficient agents in the treatment of both Gram-negative and Gram-positive biofilms (Kapoor et al., 2011; Liu et al., 2013). HDM-4 exhibits broad-spectrum inhibitory activity against biofilm formation of Gram-negative bacteria at sub-MIC levels, thus expanding its potential applications. Notably, HDM-4 exhibited strong anti-biofilm activity at the same concentration (8 μg/ml) toward four separate Gram-negative bacteria, suggesting that the underlying mode of action against biofilms involves different mechanisms than does the killing of planktonic cells, as also concluded for cationic anti-biofilm peptides (de la Fuente-Núñez et al., 2012).

It is surprising that the structure of HDM-4, comprising only two different residues, confers properties similar to those exhibited by complex peptide sequences found in Nature. This simple template is desirable because it should reduce the cost-of-goods during large-scale synthesis. Indeed a feasible gram-scale synthesis route for peptoids has been demonstrated (Jahnsen et al., 2012).

SIGNIFICANCE

In an era in which novel antibiotic agents are greatly needed, we have characterized the activity of a host defense peptidomimetic (HDM-4) with an attractive activity profile including beneficial features such as simplicity of sequence and proteolytic stability. We have demonstrated that HDM-4 mobilizes innate immune defenses and suppresses LPS-mediated inflammation, thus reducing the risk of lethal sepsis-related inflammation while maintaining potential protective efficacy. In addition, we have shown that the compound directly fights Gram-negative bacteria in a multifunctional manner and that bacterial killing takes place because of the combined effects of membrane perturbation and targeting of intracellular components. Furthermore, we have provided evidence that this complex mode of action is less likely to confer resistance development in *E. coli* when compared to the major classes of antibiotics currently used in the clinic, and that activity against multiresistant bacterial biofilms is an added asset. The traditional issues

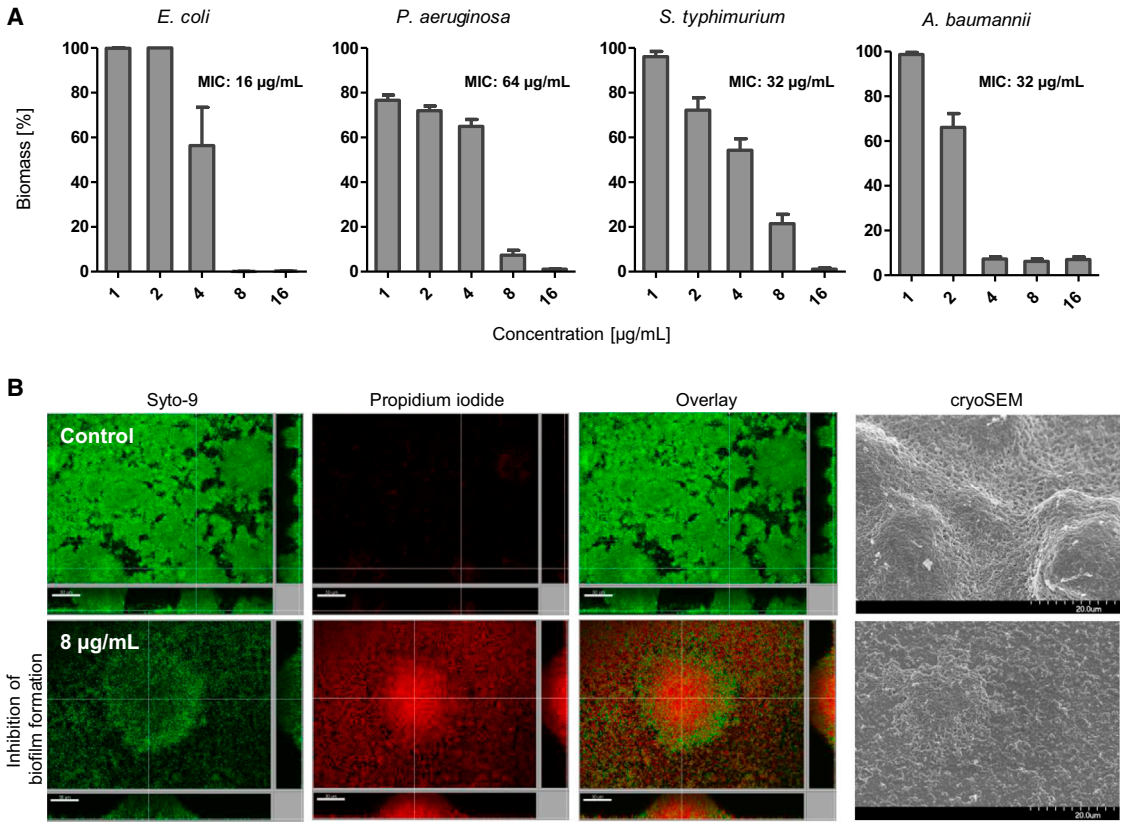

Figure 4. Anti-Biofilm Activity

(A) Inhibition of biofilm formation by various Gram-negative bacteria. The planktonic cell MIC in the biofilm media is given for each strain in the respective panel. The bars represent the percentage of the biomass after 24 hr of treatment with HDM-4 at different concentrations as compared to an untreated biofilm. Data are represented as mean ± SEM.

(B) Antibiofilm activity of HDM-4 investigated by flow cell analysis of *P. aeruginosa* (PA14). Biofilm was grown in flow cells for 144 hr with continuous treatment with 8 μg/ml (i.e., 0.125 × MIC) HDM-4 prior to live/dead staining (Syto-9 for green-staining of all cells and propidium iodide for red-staining of dead cells) followed by imaging by confocal laser-scanning microscopy (CLSM) and cryo scanning-electron microscopy. For CLSM micrographs, the scale bars represent 30 μm, and the central pictures show horizontal optical sections, while the flanking pictures show vertical optical sections.

encountered during antibiotic and HDP development included resistance, toxicity, stability, and cost. HDM-4 provides advantageous properties for each of these criteria and consequently, has high potential as a future anti-infective drug candidate.

EXPERIMENTAL PROCEDURES

Synthesis of HDM-4 and Its Tagged Variant

HDM-4 was prepared by automated MW-assisted solid-phase peptide synthesis on a CEM Liberty microwave peptide synthesizer as previously described (Jahnsen et al., 2012). The fluorescent tag was introduced prior to cleavage from the solid phase. Tagging conditions involved the use of 5 equivalents of 5(6)-carboxy-tetramethylrhodamine (Merck), 5 equivalents of diisopropyl carbodiimide (Iris Biotech), and 5 equivalents of 1-hydroxy-7-aza-benzotriazole (TCI) in the solvent DMF (VWR), with treatment at room temperature, overnight.

Bacterial Strains

Several Gram-negative bacteria were included in the evaluation of the antibacterial activity of HDM-4 including *E. coli* O157:H7, DC2 (Clark, 1984) and DH5α (Haney et al., 2013), *P. aeruginosa* PA14 (Liberati et al., 2006), *S. enterica ssp* Typhimurium 14028S (Fields et al., 1989), multidrug-resistant *A. baumannii* Sentry C8 (Arroyo et al., 2011), and *K. pneumoniae* ATCC 13883.

Antimicrobial Activity

MICs were determined using the broth microdilution method as previously described (Jahnsen et al., 2012), with minor modifications. In brief, fresh overnight colonies were diluted 1:500 in Mueller Hinton (MH) broth II (Difco). An aliquot (100 μl) of bacterial suspension was added to the wells of a polypropylene microtiter tray (Costar) containing 11 μl of a 10-fold concentration of the desired test compound in 2-fold serial dilutions. The trays were incubated at 37°C for 24 hr. The MIC was determined as the lowest concentration showing no visible growth. All measurements were carried out three times independently in triplicate.

Killing Kinetics

The killing kinetics of *E. coli* O157:H7 by HDM-4 at various concentrations were investigated, and at 4× MIC HDM-4 was compared to imipenem (Merck), cefotaxime (Sigma), ciprofloxacin (Sigma), and polymyxin B (Sigma). Cultures were allowed to grow to exponential phase (optical density 600 [OD_{600}] of ~0.5), and were then diluted to 3.5–5.5 × 10^6 CFU/ml in MH broth II, challenged with test compound, and incubated at 37°C. Residual colony counts were determined after 0.5, 1, 2, 3, and 6 hr by plating for single colonies on MH broth II agar. All measurements were carried out in triplicate.

Outer Membrane Depolarization

The effect of HDM-4 on the permeability of the outer membrane in *E. coli* O157:H7 was evaluated by the NPN-assay (Hancock et al., 1991; Hancock

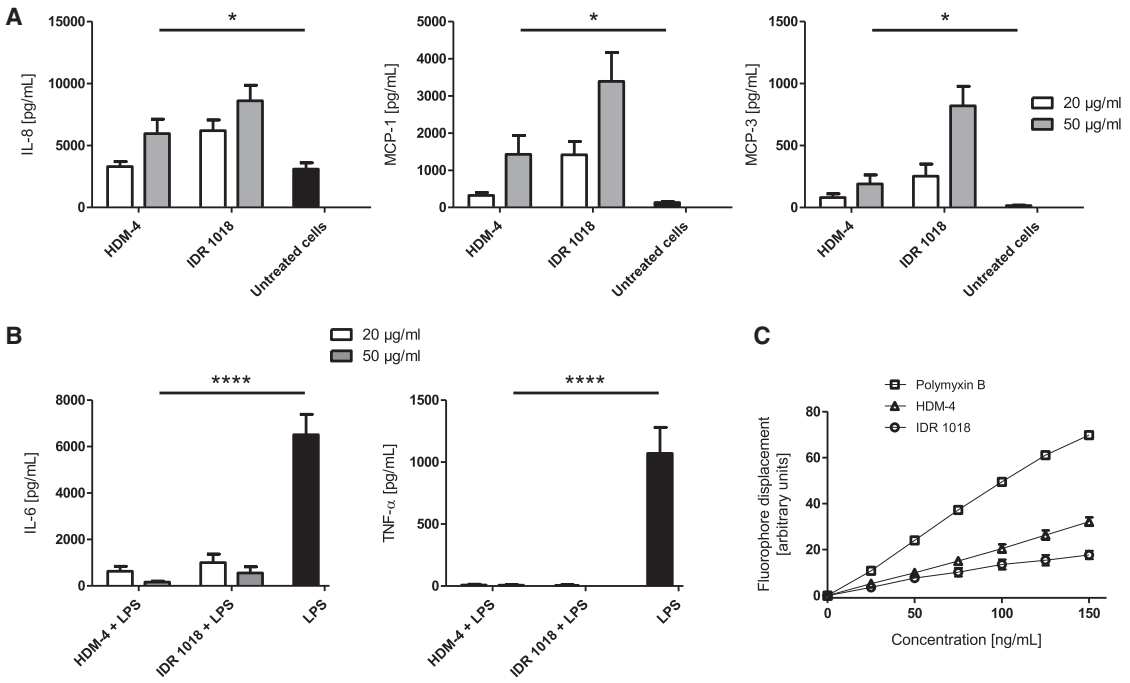

Figure 5. Immunomodulatory Activity of HDM-4

(A) Immunomodulatory activity of HDM-4 as compared to the strongly immunomodulatory peptide IDR-1018. The bars demonstrate the induction of various neutrophil and monocyte chemoattractants in human PBMCs over 24 hr during treatment with two different concentrations. Data are represented as mean ± SEM.

(B) Anti-endotoxin activity of HDM-4 as compared to that of IDR-1018. Human PBMCs were treated with two different concentrations of the compounds prior to addition of 10 ng/ml *P. aeruginosa* LPS. The activity was measured as the reduced secretion of two pro-inflammatory cytokines over 24 hr. Data are represented as mean ± SEM.

(C) LPS-binding activity as measured by the displacement of Oregon Green-tagged polymyxin B from LPS. Data are represented as mean ± SEM.

and Wong, 1984; Loh et al., 1984) measuring the uptake of 1-N-phenylnapthylamine (NPN) into the bacterial cytoplasmic membrane. The experiment was performed three times.

Inner Membrane Depolarization

Depolarization of the inner membrane was investigated by the $diSC_3$-5 (Molecular Probes) assay as previously described (Wu et al., 1999) and later modified (Chongsiriwatana and Barron, 2010). All measurements of the increase in $diSC_3$-5 fluorescence as an assessment of membrane depolarization were carried out three times.

Imaging of Membrane Damage

Membrane damage on *E. coli* O157:H7 exerted by HDM-4 was demonstrated with field emission scanning-electron microscopy. Bacterial cultures were grown to the exponential phase, and were then diluted to 2-5 × 10^7 CFU/ml in MH broth II as determined by plate counting. The bacteria were pelleted and resuspended in 0.1 M sodium cacodylate (Fluka) buffer (pH 7.4) containing the test compound. The bacteria were treated for 30 min at 23°C prior to fixation with 2.5% glutaraldehyde for 1 hr. Subsequently, the cells were loaded onto a 0.2 μm membrane filter (Whatman Nuclopore Track) using a syringe. The cells were washed with cacodylate buffer, and were then contrasted with 1% osmium tetroxide. The cells were washed with water and dehydrated by using ethanol and nitrogen critical point drying. The specimens were mounted onto stubs with Pelco conductive silver glue and coated with 5 nm gold/palladium using a sputter coater. The images were obtained on a Hitachi S4700 SEM operated at 5 kV and 10 μA at 5.0 mm working distance.

Imaging of Treated *E. coli* by Confocal Laser Scanning Microscopy

Localization of HDM-4 in *E. coli* (O157:H7) cells was investigated with TAMRA-tagged HDM-4 using confocal laser-scanning microscopy. Bacterial cultures were grown in MH broth II to reach exponential phase, and were then diluted to 3.93 × 10^7 CFU/ml as determined by plate counting. The cells were pelleted and resuspended in 5 mM PBS buffer (as tablets from Sigma: 0.01 M phosphate, 2.7 mM KCl, 0.137 M NaCl, and pH 7.4) containing the test compound. The bacteria were treated for 30 min at 37°C in the dark prior to fixation with 2.5% glutaraldehyde (Alfa Aesar) for 1 hr at 23°C in the dark. The cells were washed twice with PBS buffer, pelleted, and resuspended in PBS buffer containing 10 μg/ml DAPI. The cells were rested for 1 hr at 23°C in the dark. A drop of the bacterial suspension was placed on a coverslip, and imaging of the specimen was carried out with a Zeiss LSM 780 inverted confocal laser-scanning microscopy equipped with lasers for DAPI excitation at 405 nm and TAMRA at 543 nm. Image processing was carried out by using Fiji ImageJ 1.47q. Blue DAPI was falsely colored green and red TAMRA was falsely colored magenta.

DNA Binding Assay

Binding of HDM-4 to plasmid DNA was investigated by using an agarose gel-retardation assay for evaluation of antimicrobial peptide binding to DNA as previously described (Haney et al., 2013) with modifications. Unmodified pUCP19 plasmid was purified from an overnight culture of *E. coli* (DH5α/pUCP19) cells using a Plasmid Purification Kit (QIAGEN Inc.). Water was used to elute the pUCP19 vector, and the concentration of the purified plasmid was determined by using a NanoDrop machine (NanoDrop Products). Plasmid (200 ng) was incubated at 23°C with increasing amounts of HDM-4 in 20 μl of binding buffer (5% glycerol, 10 mM Tris–HCl at pH 8.0, 1 mM EDTA, 1 mM dithioreitol, 20 mM KCl, and 50 μg/ml BSA). After 1 hr of incubation, 2 μl of 10× loading buffer (Invitrogen) was added to the mixture. Half of this sample (i.e., 100 ng of plasmid) was loaded onto a 1% agarose gel in Tris-acetate-EDTA (TAE) buffer containing SYBR Safe DNA gel stain (Invitrogen). The gel was run at 100 V for approximately 45 min and the DNA bands were depicted with UV light using a Chemigenius 2 Bio Imaging System (Syngene).

Resistance Development

Sublethal treatment of *E. coli* O157:H7 with HDM-4, imipenem, cefotaxime, ciprofloxacin, and polymyxin B was carried out as follows: initially, bacteria from the same subculture were plated and treated with test compound as for regular MIC determination. The following day, OD_{600} was measured. From the well with the lowest concentration where >50% loss of OD_{600} could be detected, bacteria were diluted 1:20 and plated anew. This step was repeated until the bacteria were exposed to a total of 20 sublethal treatments. Bacteria without treatment were plated in parallel. After 20 cycles, MIC was determined as described, and data for treated subcultures were compared to the nontreated subculture. The treated subcultures were grown in test tubes for two cycles, and then MIC comparison was repeated. All MIC determinations were carried out in three independent determinations.

Isolation of Peripheral Blood Mononuclear Cells

Blood from healthy adult volunteers was collected (upon informed consent) in sodium heparin anticoagulant collection tubes (BD Biosciences), in accordance with University of British Columbia ethics permission and guidelines. The blood was diluted 1:1 with PBS buffer, pH 7. Blood cells were separated over Ficoll-Paque (GE Healthcare) by centrifugation (Beckman Coulter Allegra 6R) for 20 min at 1,450 rpm. The PBMCs were collected and washed twice with PBS. The cells were then resuspended in complete RPMI 1640 medium (Hyclone) supplemented with 10% FBS (Invitrogen) and quantified for viable cells by Trypan blue (Sigma) exclusion on a Zeiss light microscope.

Treatment of PBMCs

PBMCs were diluted to 1×10^6 cells/ml in RPMI 1640 medium supplemented with 10% FBS and seeded into a 48-well plate (Costar) with 500 μl in each well. The cells were then left in the incubator for 2 hr at 37°C in 5% CO_2. The cells were then treated with HDM-4 or IDR-1018 at both 20 μg/ml and 50 μg/ml. As a negative control, 2% Triton X-100 was used. In experiments aimed at determining the LPS-neutralizing effect of HDM-4, *Pseudomonas aeruginosa* strain H103 LPS was added to give a final concentration of 10 ng/ml. After 24 hr of exposure at 37°C in 5% CO_2, the content of each well was transferred to an Eppendorf tube, and then the cells were pelleted (Thermo Electron Legend Micro 21) at 2,000 rpm for 10 min. The supernatants were aliquoted and stored at −20°C before cytokine or LDH determinations. All treatments were carried out twice.

LDH Assay

Peptide toxicity against PBMCs was assessed by determining the release of LDH into the supernatant upon treatment, as previously described (Decker and Lohmann-Matthes, 1988). The assay was carried out five times in duplicate.

ELISA

The levels of various chemokines comprising IL-8, MCP-1, and MCP-3 as well as the pro-inflammatory cytokines IL-6 and TNF-α were detected by using a sandwich ELISA method and eBiosciences kits (Invitrogen, R&D Systems). All ELISAs were carried out in duplicate on at least five biological replicates.

LPS Binding

LPS binding was investigated by Oregon Green-tagged polymyxin fluorophore displacement as previously described (Moore et al., 1986) using 4 μg *Pseudomonas aeruginosa* PAO1 strain H103 LPS. Polymyxin B was used as a positive control while buffer was used as a negative control. All titrations were carried out three times.

Inhibition of Biofilm Formation

Screening for antibiofilm activity was performed in a microtiter plate assay as previously described (Pitts et al., 2003) with minor modifications (de la Fuente-Núñez et al., 2012). In brief, fresh overnight cultures were diluted in the following manner: *E. coli* 1:100 in Lennox broth (LB; Fisher Scientific): *P. aeruginosa* 1:100 in LB, *S. typhimurium* 1:10 in BM2 glucose medium—62 mM potassium phosphate buffer (pH 7), 7 mM $(NH_4)_2SO_4$, 2 mM $MgSO_4$, 10 μM $FeSO_4$, 0.4% (wt/vol) glucose, and 0.5% casamino acids (BDH, Fisher and Sigma)—and *A. baumannii* 1:10 in LB (Difco). An aliquot (100 μl) of this bacterial suspension was added to the wells of a polypropylene microtiter plate (Costar) containing 11 μl of ten times the desired final concentration of test compound in 2-fold serial dilutions. After incubation at 37°C for 24 hr, adherent biofilm was determined by the crystal violet staining method. The experiment was carried out in triplicate.

Flow Cell Experiments and Biofilm Imaging by Confocal and Cryo-Scanning-Electron Microscopy

The flow cell cultivation was carried out as previously described (de la Fuente-Núñez et al., 2012) with modifications. In brief, fresh overnight cultures of *P. aeruginosa* PA14 were diluted to $1.5–7.5 \times 10^8$ CFU/ml in LB as determined by plate counts. Then 400 μl of bacterial suspension was injected into each channel of a three-channel flow cell (IBI scientific), and subsequently the cells were allowed to adhere for 2 hr. A continuous flow of BM2 medium with or without 8 μg/ml HDM-4 at 3.6 ml/hr was applied to the channels, and the biofilm was grown for 144 hr with a setup consisting of Pharmacia LBK pumps and sterilized silicon tubing (VWR). After cultivation, the biofilm was stained with 1 μM Syto-9 (Invitrogen) and 5 μM propidium iodide (Invitrogen) in 0.9% NaCl. Imaging was carried out on an Olympus FV-1000 inverted confocal laser-scanning microscope equipped with lasers for green Syto-9 excitation at 488 nm and red propidium iodide excitation at 568 nm. Three-dimensional reconstruction was carried out in Imaris Bitplane software.

After undergoing confocal microscopy, the specimen was fixed with 2.5% glutaraldehyde and depicted with CryoSEM. Small pieces of each flow cell coverslip were excised with a diamond cutter, mounted onto a stub, and plunge-frozen in liquid nitrogen. The stub was transferred to continuous vacuum conditions in a CryoSEM sample preparation container (Emitech K1250). The temperature was increased to −95°C and decreased to −138°C through a 20 min time span to sublimate any condensed water. The sample was coated with 5 nm platinum and transferred to a Hitachi S4700 SEM operated at 5 kV and 10 μA at 12.5–15.0 mm working distance with a 30% specimen tilt.

Statistical Analysis

Statistical analyses were carried out using Graphpad Prism 5 software. All standard curves had R squared values of >0.95 and at least five data points. Data sets were compared with Student's t test for paired data sets and ANOVA for multiple data sets. All data described as significant had at least a 95% confidence interval: *$p \leq 0.5$. ****$p \leq 0.0001$.

ACKNOWLEDGMENTS

We thank Derrick Horne for assistance in the electron microscopy imaging. We thank Ashley Hilchie and Laurence Madera for assistance in blood collection. We thank Fany Reffuveille for providing recommendations for bacterial growth conditions in the crystal violet assay. Finally, we thank Jelena Pistolic for technical assistance. The present work was performed as part of the Danish Centre for Antibiotic Research and Development financed by The Danish Council for Strategic Research (grant no. 09-067075). Funding for research in the lab of R.E.W.H. was provided by the Canadian Institutes of Health Research (CIHR). E.F.H. is supported by a postdoctoral fellowship from the CIHR. R.E.W.H. holds a Canada Research Chair.

Received: August 7, 2013
Revised: September 8, 2013
Accepted: September 13, 2013
Published: October 10, 2013

REFERENCES

Arroyo, L.A., Herrera, C.M., Fernandez, L., Hankins, J.V., Trent, M.S., and Hancock, R.E.W. (2011). The pmrCAB operon mediates polymyxin resistance in *Acinetobacter baumannii* ATCC 17978 and clinical isolates through phosphoethanolamine modification of lipid A. Antimicrob. Agents Chemother. *55*, 3743–3751.

Boucher, H.W., Talbot, G.H., Bradley, J.S., Edwards, J.E., Gilbert, D., Rice, L.B., Scheld, M., Spellberg, B., and Bartlett, J. (2009). Bad bugs, no drugs: no ESKAPE! An update from the Infectious Diseases Society of America. Clin. Infect. Dis. *48*, 1–12.

Bowdish, D.M.E., Davidson, D.J., and Hancock, R.E.W. (2005). A re-evaluation of the role of host defence peptides in mammalian immunity. Curr. Protein Pept. Sci. *6*, 35–51.

Brogden, K.A. (2005). Antimicrobial peptides: pore formers or metabolic inhibitors in bacteria? Nat. Rev. Microbiol. *3*, 238–250.

Chongsiriwatana, N., and Barron, A. (2010). Comparing bacterial membrane interactions of antimicrobial peptides and their mimics. Methods Mol Biol. *618*, 171–182.

Clark, D. (1984). Novel antibiotic hypersensitive mutants of *Escherichia coli* genetic mapping and chemical characterization. FEMS Microbiol. Lett. *21*, 189–195.

Costerton, J.W., Stewart, P.S., and Greenberg, E.P. (1999). Bacterial biofilms: a common cause of persistent infections. Science *284*, 1318–1322.

Davies, M.G., and Hagen, P.O. (1997). Systemic inflammatory response syndrome. Br. J. Surg. *84*, 920–935.

de la Fuente-Núñez, C., Korolik, V., Bains, M., Nguyen, U., Breidenstein, E.B.M., Horsman, S., Lewenza, S., Burrows, L., and Hancock, R.E.W. (2012). Inhibition of bacterial biofilm formation and swarming motility by a small synthetic cationic peptide. Antimicrob. Agents Chemother. *56*, 2696–2704.

Decker, T., and Lohmann-Matthes, M.-L. (1988). A quick and simple method for the quantitation of lactate dehydrogenase release in measurements of cellular cytotoxicity and tumor necrosis factor (TNF) activity. J. Immunol. Methods *115*, 61–69.

Donlan, R.M. (2001). Biofilm formation: a clinically relevant microbiological process. Clin. Infect. Dis. *33*, 1387–1392.

Fields, P.I., Groisman, E.A., and Heffron, F. (1989). A *Salmonella* locus that controls resistance to microbicidal proteins from phagocytic cells. Science *243*, 1059–1062.

Fjell, C.D., Hiss, J.A., Hancock, R.E.W., and Schneider, G. (2012). Designing antimicrobial peptides: form follows function. Nat. Rev. Drug Discov. *11*, 37–51.

Gallo, R.L., Kim, K.J., Bernfield, M., Kozak, C.A., Zanetti, M., Merluzzi, L., and Gennaro, R. (1997). Identification of CRAMP, a cathelin-related antimicrobial peptide expressed in the embryonic and adult mouse. J. Biol. Chem. *272*, 13088–13093.

Hale, J.D., and Hancock, R.E.W. (2007). Alternative mechanisms of action of cationic antimicrobial peptides on bacteria. Expert Rev. Anti-Infect. *5*, 951–959.

Hancock, R.E.W., and Wong, P.G. (1984). Compounds which increase the permeability of the *Pseudomonas aeruginosa* outer membrane. Antimicrob. Agents Chemother. *26*, 48–52.

Hancock, R.E.W., and Sahl, H.G. (2006). Antimicrobial and host-defense peptides as new anti-infective therapeutic strategies. Nat. Biotechnol. *24*, 1551–1557.

Hancock, R.E.W., Farmer, S.W., Li, Z.S., and Poole, K. (1991). Interaction of aminoglycosides with the outer membranes and purified lipopolysaccharide and OmpF porin of *Escherichia coli*. Antimicrob. Agents Chemother. *35*, 1309–1314.

Haney, E.F., Petersen, A.P., Lau, C.K., Jing, W., Storey, D.G., and Vogel, H.J. (2013). Mechanism of action of puroindoline derived tryptophan-rich antimicrobial peptides. Biochim. Biophys. Acta *1828*, 1802–1813.

Hilpert, K., Volkmer-Engert, R., Walter, T., and Hancock, R.E.W. (2005). High-throughput generation of small antibacterial peptides with improved activity. Nat. Biotechnol. *23*, 1008–1012.

HsuChen, C.C., and Feingold, D.S. (1973). The mechanism of polymyxin B action and selectivity toward biologic membranes. Biochemistry *12*, 2105–2111.

Jabes, D. (2011). The antibiotic R&D pipeline: an update. Curr. Opin. Microbiol. *14*, 564–569.

Jahnsen, R.D., Frimodt-Møller, N., and Franzyk, H. (2012). Antimicrobial activity of peptidomimetics against multidrug-resistant *Escherichia coli*: a comparative study of different backbones. J. Med. Chem. *55*, 7253–7261.

Kapoor, R., Wadman, M.W., Dohm, M.T., Czyzewski, A.M., Spormann, A.M., and Barron, A.E. (2011). Antimicrobial peptoids are effective against *Pseudomonas aeruginosa* biofilms. Antimicrob. Agents Chemother. *55*, 3054–3057.

Liberati, N.T., Urbach, J.M., Miyata, S., Lee, D.G., Drenkard, E., Wu, G., Villanueva, J., Wei, T., and Ausubel, F.M. (2006). An ordered, nonredundant library of *Pseudomonas aeruginosa* strain PA14 transposon insertion mutants. Proc. Natl. Acad. Sci. USA *103*, 2833–2838.

Liu, Y., Knapp, K.M., Yang, L., Molin, S., Franzyk, H., and Folkesson, A. (2013). High in vitro antimicrobial activity of β-peptoid-peptide hybrid oligomers against planktonic and biofilm cultures of *Staphylococcus epidermidis*. Int. J. Antimicrob. Agents *41*, 20–27.

Loh, B., Grant, C., and Hancock, R.E.W. (1984). Use of the fluorescent probe 1-N-phenylnaphthylamine to study the interactions of aminoglycoside antibiotics with the outer membrane of *Pseudomonas aeruginosa*. Antimicrob. Agents Chemother. *26*, 546–551.

Mookherjee, N., and Hancock, R.E.W. (2007). Cationic host defence peptides: innate immune regulatory peptides as a novel approach for treating infections. Cell. Mol. Life Sci. *64*, 922–933.

Mookherjee, N., Brown, K.L., Bowdish, D.M.E., Doria, S., Falsafi, R., Hokamp, K., Roche, F.M., Mu, R.X., Doho, G.H., Pistolic, J., et al. (2006). Modulation of the TLR-mediated inflammatory response by the endogenous human host defense peptide LL-37. J. Immunol. *176*, 2455–2464.

Moore, R.A., Bates, N.C., and Hancock, R.E.W. (1986). Interaction of polycationic antibiotics with *Pseudomonas aeruginosa* lipopolysaccharide and lipid A studied by using dansyl-polymyxin. Antimicrob. Agents Chemother. *29*, 496–500.

Oteo, J., Pérez-Vázquez, M., and Campos, J. (2010). Extended-spectrum [β]-lactamase producing *Escherichia coli*: changing epidemiology and clinical impact. Curr. Opin. Infect. Dis. *23*, 320–326.

Parsek, M.R., and Singh, P.K. (2003). Bacterial biofilms: an emerging link to disease pathogenesis. Annu. Rev. Microbiol. *57*, 677–701.

Peschel, A., and Sahl, H.-G. (2006). The co-evolution of host cationic antimicrobial peptides and microbial resistance. Nat. Rev. Microbiol. *4*, 529–536.

Pitts, B., Hamilton, M.A., Zelver, N., and Stewart, P.S. (2003). A microtiter-plate screening method for biofilm disinfection and removal. J. Microbiol. Methods *54*, 269–276.

Römling, U., and Balsalobre, C. (2012). Biofilm infections, their resilience to therapy and innovative treatment strategies. J. Intern. Med. *272*, 541–561.

Scott, M.G., Vreugdenhil, A.C.E., Buurman, W.A., Hancock, R.E.W., and Gold, M.R. (2000). Cutting edge: cationic antimicrobial peptides block the binding of lipopolysaccharide (LPS) to LPS binding protein. J. Immunol. *164*, 549–553.

Scott, M.G., Davidson, D.J., Gold, M.R., Bowdish, D., and Hancock, R.E.W. (2002). The human antimicrobial peptide LL-37 is a multifunctional modulator of innate immune responses. J. Immunol. *169*, 3883–3891.

Scott, M.G., Dullaghan, E., Mookherjee, N., Glavas, N., Waldbrook, M., Thompson, A., Wang, A.K., Lee, K., Doria, S., Hamill, P., et al. (2007). An anti-infective peptide that selectively modulates the innate immune response. Nat. Biotechnol. *25*, 465–472.

Sieprawska-Lupa, M., Mydel, P., Krawczyk, K., Wójcik, K., Puklo, M., Lupa, B., Suder, P., Silberring, J., Reed, M., Pohl, J., et al. (2004). Degradation of human antimicrobial peptide LL-37 by *Staphylococcus aureus*-derived proteinases. Antimicrob. Agents Chemother. *48*, 4673–4679.

Singh, P.K., Schaefer, A.L., Parsek, M.R., Moninger, T.O., Welsh, M.J., and Greenberg, E.P. (2000). Quorum-sensing signals indicate that cystic fibrosis lungs are infected with bacterial biofilms. Nature *407*, 762–764.

Storm, D.R., Rosenthal, K.S., and Swanson, P.E. (1977). Polymyxin and related peptide antibiotics. Annu. Rev. Biochem. *46*, 723–763.

Theuretzbacher, U. (2013). Global antibacterial resistance: The never-ending story. J. Global Antibiot. Res. *1*, 63–69.

Turner-Brannen, E., Choi, K.Y., Lippert, D.N.D., Cortens, J.P., Hancock, R.E.W., El-Gabalawy, H., and Mookherjee, N. (2011). Modulation of interleukin-1β-induced inflammatory responses by a synthetic cationic innate defence regulator peptide, IDR-1002, in synovial fibroblasts. Arthritis Res. Ther. *13*, R129.

Wieczorek, M., Jenssen, H., Kindrachuk, J., Scott, W.R.P., Elliott, M., Hilpert, K., Cheng, J.T.J., Hancock, R.E.W., and Straus, S.K. (2010). Structural studies of a peptide with immune modulating and direct antimicrobial activity. Chem. Biol. *17*, 970–980.

Wu, M., Maier, E., Benz, R., and Hancock, R.E.W. (1999). Mechanism of interaction of different classes of cationic antimicrobial peptides with planar bilayers and with the cytoplasmic membrane of *Escherichia coli*. Biochemistry *38*, 7235–7242.